Geochemical Perspectives Letters

Black shale Mo isotope record reveals dynamic ocean redox during the Mesoproterozoic Era

Y. Ye[1,2], S. Zhang[2*], H. Wang[2], X. Wang[2], C. Tan[2], M. Li[3], C. Wu[1], D.E. Canfield[2,4]

doi: 10.7185/geochemlet.2118

Abstract

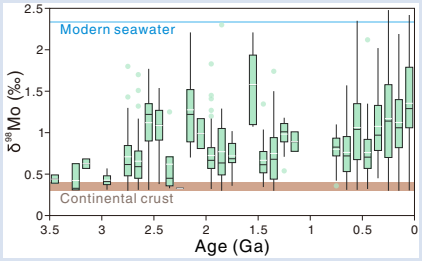

Eukaryotes reached ecological importance in the late Neoproterozoic Era, some one billion years after their emergence. Their slow rise to prominence has been ascribed to prolonged environmental stagnation, but testing this idea requires an appraisal of the evolution of atmospheric and ocean chemistry. Establishing a nuanced geochemical history is, however, challenging due to the paucity of well preserved sedimentary rocks. Here, we present new Mo isotope ratios from black shale units spanning ~1560 to ~1170 Ma. These results, combined with literature data, reveal potential episodic expansions of oxygenated and/or mildly reducing conditions during the Mesoproterozoic Era, suggesting fluctuating oxygen availability that could have exerted a crucial control on the evolution of eukaryotes.

Received 17 January 2021 | Accepted 27 April 2021 | Published 15 June 2021

Introduction

The Mesoproterozoic Era has been described as a time of climatic, geochemical, and biological stasis. The relatively small carbonate carbon isotope variations and the absence of continental ice sheets contrast starkly with the following Neoproterozoic Era when low latitude glaciations and huge carbon isotope excursions were prevalent. Neoproterozoic marine environments also witnessed the diversification of eukaryotic phytoplankton and animals, which have long been linked to the surface oxygenation, while low oxygen availability in Mesoproterozoic oceans may have limited eukaryotic diversity and organismal complexity, generating a sluggish biosphere (Anbar and Knoll, 2002). This traditional view, however, is evolving with a growing amount of newly reported Mesoproterozoic fossils, such as the filamentous and lobate fossils, interpreted as probable crown group red algae, in the ~1600 Ma Tirohan Dolomite of central India (Bengtson *et al.*, 2017) and the ~1560 Ma Gaoyuzhuang carbonaceous compressions closely resembling modern benthic algae (Zhu *et al.*, 2016).

If we accept the notion that life has evolved with the environment, then these biological innovations should be considered together with the redox changes in Mesoproterozoic oceans. Indeed, existing data show that Mesoproterozoic deep waters had variable redox chemistry ranging between oxic, euxinic (sulfidic), and ferruginous conditions (Wang *et al.*, 2017). Within the context of deep ocean redox fluctuations, there is a broad debate on atmospheric oxygen levels. Some studies have advocated very low concentrations of 0.1–1 % PAL (present atmospheric level; Planavsky *et al.*, 2020), yet others provided evidence for minimum values of 1–4 % PAL (Zhang *et al.*, 2016; Canfield *et al.*, 2018).

To develop and test these ideas, we present total organic carbon (TOC), Fe speciation, Mo abundance and isotopic compositions (denoted as $\delta^{98}Mo_{NIST3134=0.25}$; Nägler *et al.*, 2014) of shale samples from Mesoproterozoic strata spanning from ~1560 to ~1170 Ma. Our results, combined with published data, comprise the most comprehensive current Mo isotope record of Mesoproterozoic marine settings and a valuable window into state of ocean redox.

Geological Background and Samples

Samples were obtained from two drill cores in the Yanliao Basin, North China (the Gaoyuzhuang and Hongshuizhuang Formations) and from multiple outcrops of the Shennongjia Group, South China (Fig. 1). The Gaoyuzhuang Formation is composed of predominately carbonate rocks, and it can be divided into four lithological members (Shang *et al.*, 2019). Our study focuses on Member III, where organic-rich calcareous shales were deposited in a relatively deep water environment. Based on zircon U–Pb ages, the time frame of Member III is constrained to ~1580–1560 Ma (Tian *et al.*, 2015). Above the Gaoyuzhuang Formation, thick bedded dolostones of the Yangzhuang and Wumishan Formations make up the majority of the Jixian Group in North China. Subsequent transgression promoted the offshore deposition of the Hongshuizhuang

1. Key Laboratory of Orogenic Belts and Crustal Evolution, Ministry of Education, School of Earth and Space Sciences, Peking University, Beijing 100871, China
2. Key Laboratory of Petroleum Geochemistry, Research Institute of Petroleum Exploration and Development, China National Petroleum Corporation, Beijing 100083, China
3. School of Geophysics and Information Technology, China University of Geosciences, Beijing 100083, China
4. Department of Biology and Nordcee, University of Southern Denmark, Odense M 5230, Denmark
* Corresponding author (email: sczhang@petrochina.com.cn)

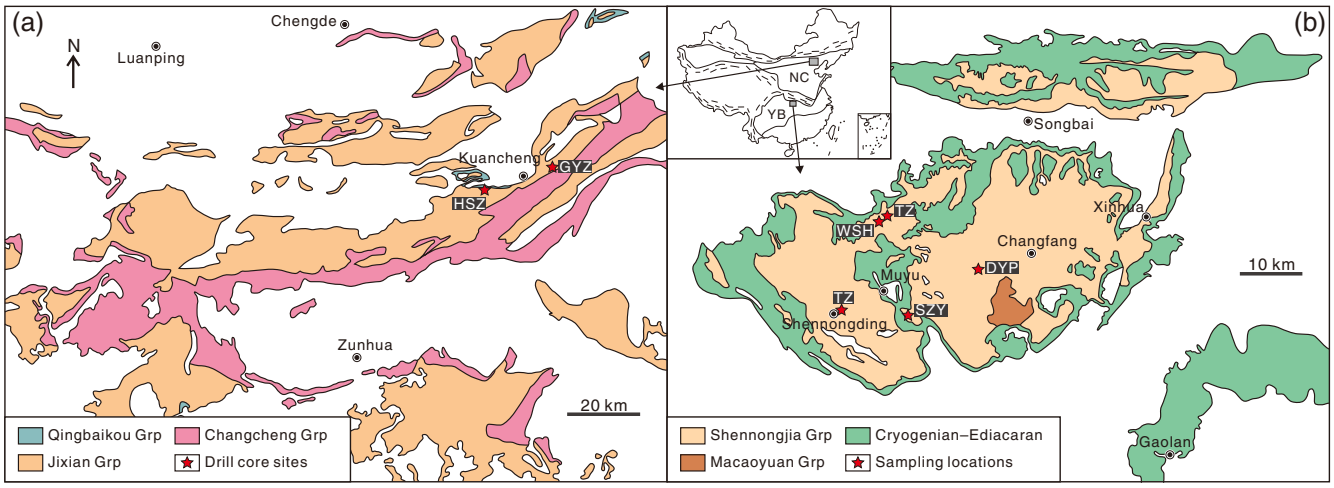

Figure 1 Maps showing the Proterozoic outcrops in the **(a)** Yanliao and **(b)** Shennongjia regions. Sampling locations are marked as stars. Formations: GYZ, Gaoyuzhuang; HSZ, Hongshuizhuang; DYP, Dayanping; TZ, Taizi; WSH, Wenshuihe; SZY, Songziyuan.

shales. No radiometric dating has been conducted for the Hongshuizhuang Formation itself, but U–Pb ages of ~1480 and ~1440 Ma were reported from the underlying Wumishan Formation and the overlying Tieling Formation, respectively (Li *et al.*, 2014).

The Shennongjia Group in the northern margin of the Yangtze Block has been explored geochemically for TOC, trace metals, and Cr isotopes (Canfield *et al.*, 2018). Our samples for Mo isotope analysis were collected from the Dayangping, Taizi, Wenshuihe, and Songziyuan Formations. Organic-rich sediments of the latter three formations are enriched in redox sensitive elements, similar to other Mesoproterozoic black shales (Canfield *et al.*, 2018). The base of the Shennongjia Group is estimated at ~1400 Ma, while the uppermost layers deposited after ~1100 Ma (see Canfield *et al.*, 2018, for detailed stratigraphic and chronological descriptions).

Results

Our geochemical data are illustrated in Figure 2 (see Supplementary Information for methods). Ratios of Fe_{HR}/Fe_T are relatively high (>0.38) in the Gaoyuzhuang and Hongshuizhuang Formations, but vary markedly through shales of the Shennongjia Group. Note that the Shennongjia samples are plotted sequentially by number and relative to stratigraphic position, instead of exact depth, thus the Fe_{HR}/Fe_T variation does not necessarily reflect secular change. For samples with $Fe_{HR}/Fe_T >$ 0.38, their Fe_{py}/Fe_{HR} ratios are generally <0.7, while instances of elevated Fe_{py}/Fe_{HR} (>0.7) exist in the Hongshuizhuang and Taizi Formations. Molybdenum isotope values range from −1.07 ‰ to +2.21 ‰ for the Gaoyuzhuang Formation, from −0.64 ‰ to +1.35 ‰ for the Hongshuizhuang Formation, and from −0.52 ‰ to +1.12 ‰ for the Shennongjia Group. The heaviest measured $\delta^{98}Mo$ in the Gaoyuzhuang sediments coincides with enriched TOC and Mo contents, as well as a positive swing of the Fe_{py}/Fe_{HR} profile.

Molybdenum Isotopes as a Palaeoredox Proxy

Molybdenum isotopes are a well established proxy used to reconstruct marine redox state. In modern oxygenated oceans, the isotopically heavy seawater Mo signal (~2.34 ‰) mainly results from Mo uptake onto Mn oxide particles that preferentially adsorb light Mo isotopes ($\Delta^{98}Mo_{SW-Mn\text{-}ox} = \sim 3$ ‰; Siebert *et al.*, 2003; Barling and Anbar, 2004). By contrast, in euxinic basins (often hydrographically restricted today), especially when $[H_2S]_{aq}$ exceeds 11 μM (Erickson and Helz, 2000), Mo is efficiently removed from solution into sediments. Molybdenum isotopes of these sediments can reach isotopically heavy values close to open ocean seawater values (Neubert *et al.*, 2008). Such a near quantitative Mo transfer allows the use of euxinic deposits to infer seawater Mo isotope compositions. For sediments bathed under anoxic but non-euxinic or low $[H_2S]_{aq}$-containing waters, a wide range of $\delta^{98}Mo$ is observed (with a preferential retention of light mass Mo isotopes in sediments), likely reflecting the non-quantitative trapping of dissolved Mo and complexation of Mo with metal oxides or organic matter (Kendall *et al.*, 2017).

The proportion of Fe among its geochemically reactive phases can be indicative of the redox chemistry directly above the accumulating sediments. The majority of our samples possess $Fe_{HR}/Fe_T > 0.38$ but $Fe_{py}/Fe_{HR} < 0.7$ or slightly >0.7, defining deposition under ferruginous to intermittently euxinic environments (Fig. 2; Poulton and Canfield, 2011). Since $[H_2S]_{aq}$ strongly affects the removal of Mo, it is likely that low $[H_2S]_{aq}$ would have imparted an isotope fractionation during Mo burial. Accordingly, our measured $\delta^{98}Mo$ values may provide a minimum constraint on coeval seawater composition. In addition, the low Fe_{ox}/Fe_{HR} ratios of core materials and finely distributed pyrites under scanning electron microscope suggest a minor influence of post-depositional alternation (Supplementary Information).

Mesoproterozoic Molybdenum Record from Black Shales

In order to investigate the evolution of marine oxygenation, we compare our results with published $\delta^{98}Mo$ data over geological time (Fig. 3). Our compilation reveals broad changes in global ocean redox during the Mesoproterozoic Era. Moderate $\delta^{98}Mo$ values (<1.35 ‰), including samples from the Hongshuizhuang Formation and Shennongjia Group, dominate the Mesoproterozoic shale record, but excursions to higher $\delta^{98}Mo$ values are observed in the Gaoyuzhuang ($\delta^{98}Mo_{max} = 2.21$ ‰)

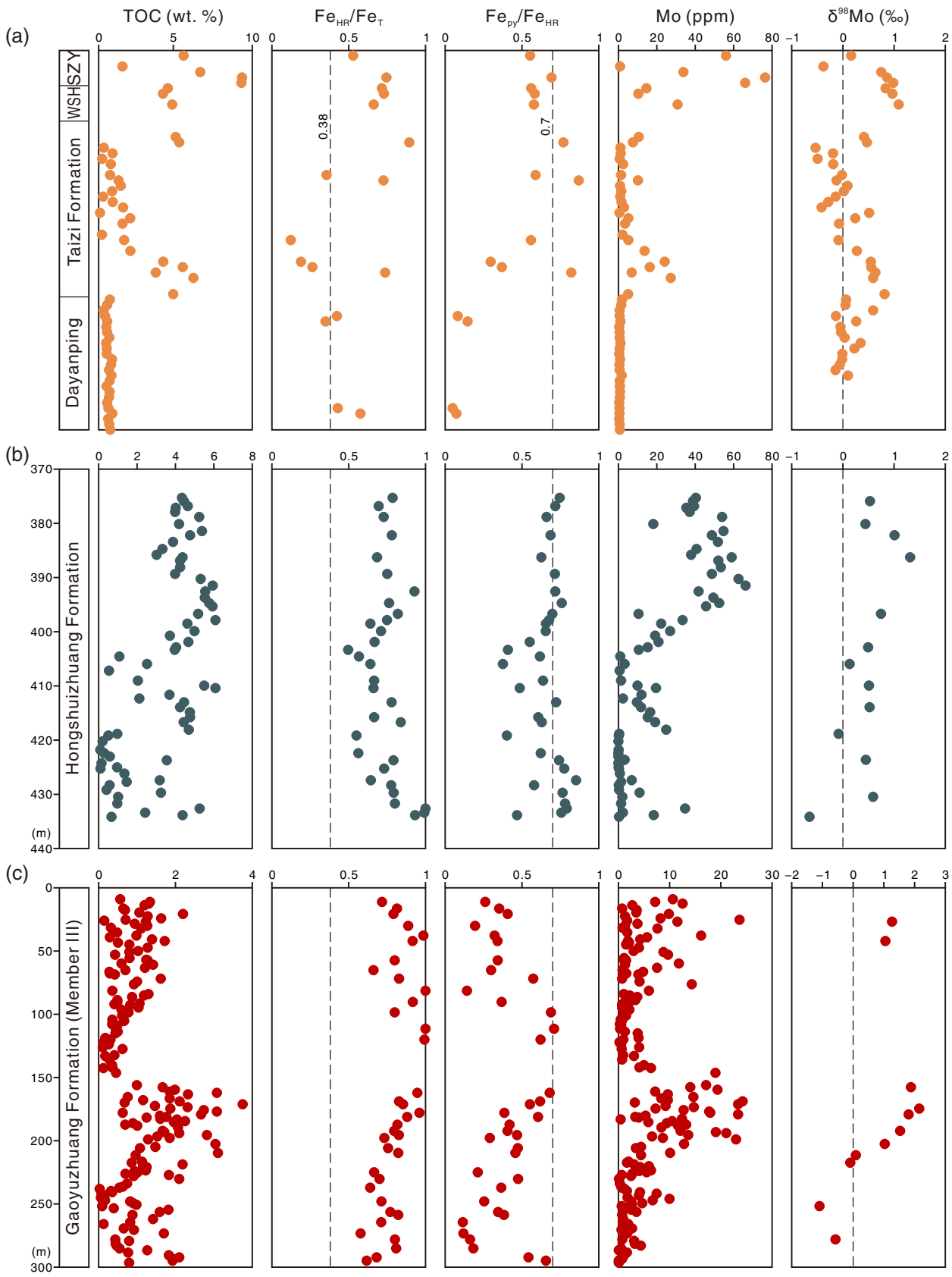

Figure 2 Geochemical profiles for shales from the **(a)** Shennongjia Group, **(b)** Hongshuizhuang Formation, and **(c)** Gaoyuzhuang Formation (Member III). The TOC and Mo contents of the Shennongjia Group are compiled from Canfield *et al.* (2018). Note that the Shennongjia samples are plotted sequentially and relative to stratigraphic position, but not as a function of depth.

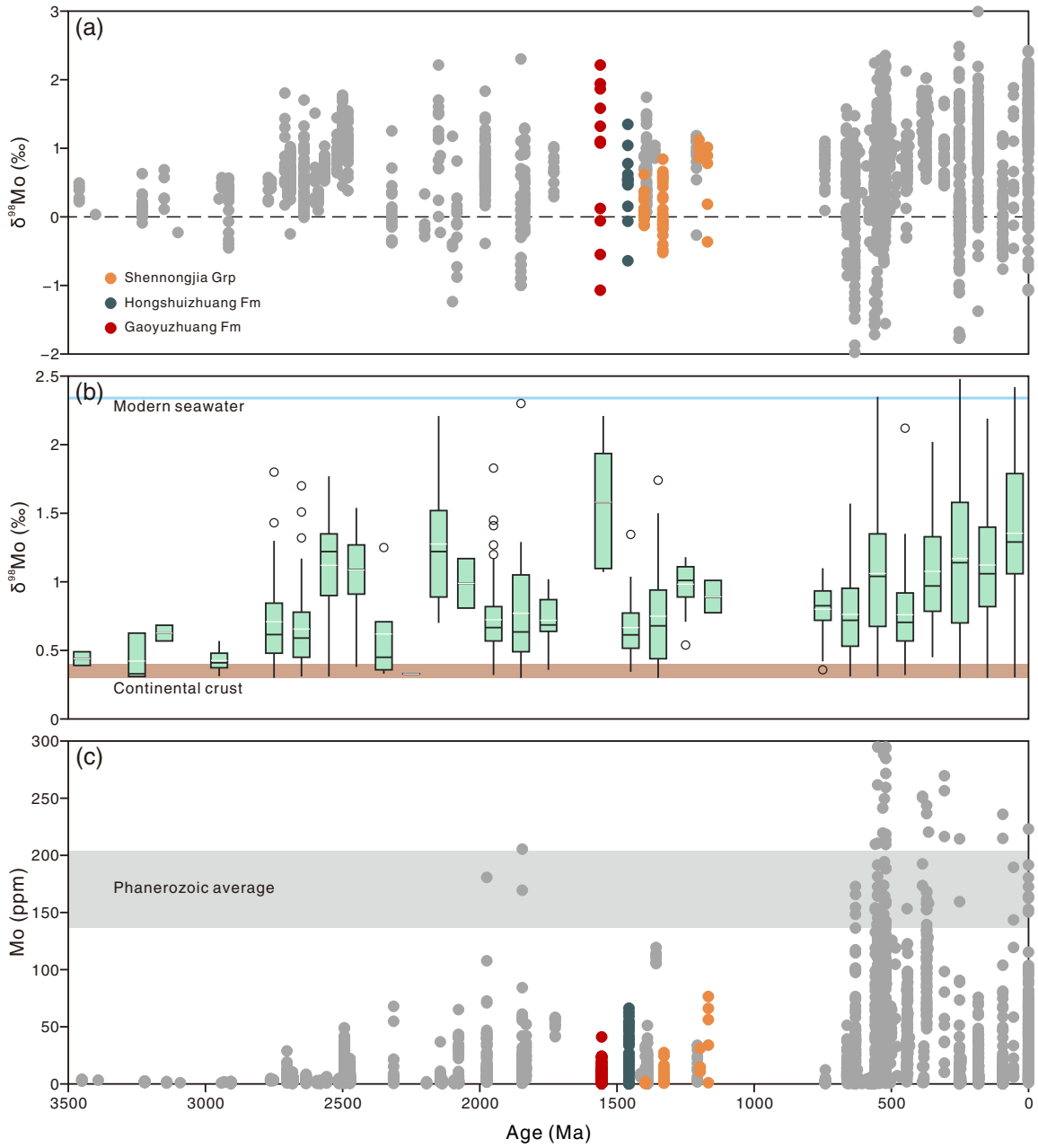

Figure 3 Black shale Mo record. **(a)** Mo isotope ratios from the Palaeoarchean to present. **(b)** Filtered data in 100 million year bins, focusing on samples with δ^{98}Mo greater than the continental crust composition (>0.3 ‰). The Box and Whisker plots show the first quartile, mean (white lines), median (black lines), third quartile, and outliers of the data. **(c)** Mo concentrations through time.

and Xiamaling Formations (~1400 Ma, $\delta^{98}Mo_{max} = 1.74$ ‰; Diamond *et al.*, 2018). On the basis of Mo isotope systematics, such heavy δ^{98}Mo values would require substantial sinks for isotopically light Mo on the seafloor. Does this mean that the ocean was at least temporarily well oxygenated during the Mesoproterozoic? We argue that these data should be interpreted cautiously and with considerations of the contemporaneous marine Mo inventory. It is expected that a well oxygenated ocean would be characterised by heavy seawater δ^{98}Mo and a large dissolved Mo reservoir (and correspondingly enhanced Mo enrichments in the few anoxic regions). We note, however, that in the Gaoyuzhuang Formation highly elevated δ^{98}Mo values occur at Mo concentrations that are much lower than Phanerozoic equivalents (Fig. 3).

The low Mo concentrations may be partly attributed to the calcareous and ferruginous nature of our Gaoyuzhuang samples. Alternatively, the elevated δ^{98}Mo values need not have been associated with the same extent of seafloor oxygenation as today. That is to say, if some intermediate redox sinks could scavenge isotopically light Mo, but with relatively high burial efficiency, elevated δ^{98}Mo values could have accompanied sedimentary Mo concentrations lower than those found in the Phanerozoic (Asael *et al.*, 2018). In the following section, we explore this scenario mathematically through the ocean Mo mass balance model.

Model for Marine Redox Distribution

At steady state, the marine Mo input flux is balanced by removal into oxic, strongly euxinic, and intermediate (mildly reducing, including oxygen minimum zones, ferruginous waters, and other

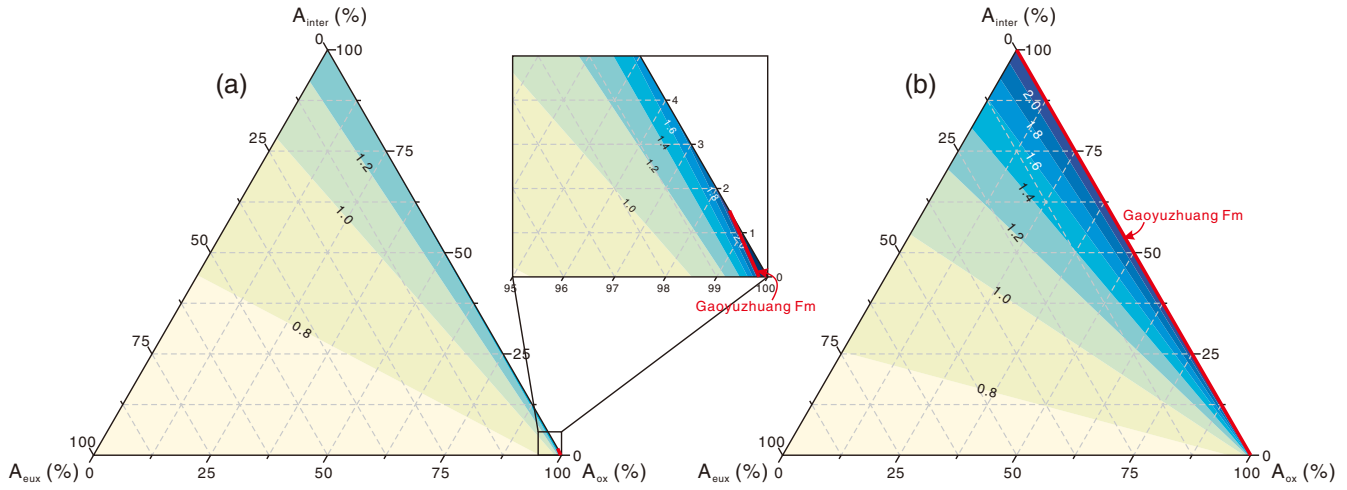

Figure 4 Estimates of ocean redox through the Mo isotope mass balance model, where A_{ox}, A_{inter}, and A_{eux} denote the seafloor areas of oxic, intermediate reducing, and strongly euxinic conditions, respectively. The left panel **(a)** is based on a fractionation of 0.7 ‰ for the intermediate sink, while the right panel **(b)** employs a larger fractionation of 1.5 ‰ for this sink.

low oxygen or intermittently euxinic settings) sinks. Of all the fractionations involved, those related to the intermediate sink are the least well constrained, yet an empirical fractionation of 0.7 ‰ is commonly chosen for this sink (Kendall *et al.*, 2017). With this isotope offset, a seawater δ^{98}Mo of 2.21 ‰, as we suggest for Member III of the Gaoyuzhuang Formation, can only be achieved with modern-like ocean oxygenation (or nearly so; Fig. 4). However, the magnitude of Mo isotope fractionation under the intermediate contexts can span the entire range between oxic and strongly euxinic end members. For example, as recently shown, ferruginous conditions can imprint greater isotope fractionation between sediments and the overlying bottom waters ($\Delta^{98}Mo_{BW-sed}$ = 0.6–2 ‰; Hutchings *et al.*, 2020). If we adjust a relatively larger factor (1.5 ‰) for the intermediate sink, the heavy δ^{98}Mo of the Gaoyuzhuang Formation can be reconciled with a line almost overlapping the A_{ox}–A_{inter} axis, which indicates either substantial oxygenated or mildly reducing water masses (Fig. 4). In the intermediate redox environments, Mo might be efficiently scavenged by organic matter, Fe oxides, or FeS colloids (Swanner *et al.*, 2020), thus in agreement with low seawater Mo concentrations as noted above.

Implications of Dynamic Ocean Redox

A growing body of ecological and geochemical evidence hints at a dynamic and patchy redox landscape for the Mesoproterozoic oceans (Zhang *et al.*, 2018; Shang *et al.*, 2019). The Mo isotope results presented here are consistent with this idea, with decided intervals indicating expanded oxygenated and/or mildly reducing waters relative to a baseline of more strongly euxinic conditions. Moreover, bootstrap resampled means of δ^{98}Mo from the Mesoproterozoic exhibit greater dispersion compared with the Phanerozoic (Supplementary Information). The recognition of redox oscillations raises critical questions about possible relationships to biological innovation. In fact, the heavy δ^{98}Mo values of the Gaoyuzhuang Formation are concurrent with body fossil evidence for macroscopic multicellular eukaryotes that lived near the storm wave base (Zhu *et al.*, 2016). If such δ^{98}Mo signatures were associated with ocean oxygenation and increasing atmospheric oxygen levels, then multicellular eukaryotes may have evolved and expanded into a permissive chemical context. Whether subsequent expansions of marine anoxic conditions have provided a hindrance to further eukaryotic evolution depends on the baseline oxygenation of the Mesoproterozoic oceans, an issue that is still unresolved. Nevertheless, future analyses of larger sample sets promise new insights into the interaction between ocean redox and bio-diversification during the Mesoproterozoic Era.

Acknowledgments

We thank Hanjie Wen for assistance with Mo isotope analyses and Gavin Foster for editorial handling. This work was funded by the National Key Research and Development Program of China (2017YFC0603101), the National Science and Technology Major Project of the Ministry of Science and Technology of China (2016ZX05004001), the Strategic Priority Research Program of the Chinese Academy of Sciences (XDA14010101), the National Natural Science Foundation of China (41530317, 41872125), and the Villum Foundation (16518). Constructive comments from Noah Planavsky and two anonymous reviewers greatly improved the manuscript.

Editor: Gavin Foster

Additional Information

Supplementary Information accompanies this letter at https://www.geochemicalperspectivesletters.org/article2118.

Cite this letter as: Ye, Y., Zhang, S., Wang, H., Wang, X., Tan, C., Li, M., Wu, C., Canfield, D.E. (2021) Black shale Mo isotope record reveals dynamic ocean redox during the Mesoproterozoic Era. *Geochem. Persp. Let.* 18, 16–21.

References

Anbar, A.D., Knoll, A.H. (2002) Proterozoic ocean chemistry and evolution: A bioinorganic bridge? *Science* 297, 1137–1142.

Asael, D., Rouxel, O., Poulton, S.W., Lyons, T.W., Bekker, A. (2018) Molybdenum record from black shales indicates oscillating atmospheric oxygen levels in the early paleoproterozoic. *American Journal of Science* 318, 275–299.

Barling, J., Anbar, A.D. (2004) Molybdenum isotope fractionation during adsorption by manganese oxides. *Earth and Planetary Science Letters* 217, 315–329.

Bengtson, S., Sallstedt, T., Belivanova, V., Whitehouse, M. (2017) Three-dimensional preservation of cellular and subcellular structures suggests 1.6 billion-year-old crown-group red algae. *PLoS Biology* 15, e2000735.

Canfield, D.E., Zhang, S., Frank, A.B., Wang, X., Wang, H., Su, J., Ye, Y., Frei, R. (2018) Highly fractionated chromium isotopes in Mesoproterozoic-aged shales and atmospheric oxygen. *Nature Communications* 9, 1–11.

Diamond, C.W., Planavsky, N.J., Wang, C., Lyons, T.W. (2018) What the ~1.4 Ga Xiamaling Formation can and cannot tell us about the mid-Proterozoic ocean. *Geobiology* 16, 219–236.

Erickson, B.E., Helz, G.R. (2000) Molybdenum(VI) speciation in sulfidic waters: Stability and lability of thiomolybdates. *Geochimica et Cosmochimica Acta* 64, 1149–1158.

Hutchings, A.M., Basu, A., Dickson, A.J., Turchyn, A.V. (2020) Molybdenum geochemistry in salt marsh pond sediments. *Geochimica et Cosmochimica Acta* 284, 75–91.

Kendall, B., Dahl, T.W., Anbar, A.D. (2017) The stable isotope geochemistry of molybdenum. *Reviews in Mineralogy and Geochemistry* 82, 683–732.

Li, H., Su, W., Zhou, H., Xiang, Z., Tian, H., Yang, L., Huff, D.W., Ettensohn, R.F. (2014) The first precise age constraints on the Jixian System of the Meso- to Neoproterozoic Standard Section of China: SHRIMP zircon U-Pb dating of bentonites from the Wumishan and Tieling formations in the Jixian Section, North China Craton. *Acta Petrologica Sinica* 30, 2999–3012 (in Chinese with English abstract).

Nägler, T.F., Anbar, A.D., Archer, C., Goldberg, T., Gordon, G.W., Greber, N.D., Siebert, C., Sohrin, Y., Vance, D. (2014) Proposal for an international molybdenum isotope measurement standard and data representation. *Geostandards and Geoanalytical Research* 38, 149–151.

Neubert, N., Nägler, T.F., Böttcher, M.E. (2008) Sulfidity controls molybdenum isotope fractionation into euxinic sediments: Evidence from the modern Black Sea. *Geology* 36, 775–778.

Planavsky, N.J., Reinhard, C.T., Isson, T.T., Ozaki, K., Crockford, P.W. (2020) Large mass-independent oxygen isotope fractionations in mid-Proterozoic sediments: Evidence for a low-oxygen atmosphere? *Astrobiology* 20, 628–636.

Poulton, S.W., Canfeld, D.E. (2011) Ferruginous conditions: A dominant feature of the ocean through Earth's history. *Elements* 7, 107–112.

Shang, M., Tang, D., Shi, X., Zhou, L., Zhou, X., Song, H., Jiang, G. (2019) A pulse of oxygen increase in the early Mesoproterozoic ocean at ca. 1.57–1.56 Ga. *Earth and Planetary Science Letters* 527, 115797.

Siebert, C., Nägler, T.F., von Blanckenburg, F., Kramers, J.D. (2003) Molybdenum isotope records as a potential new proxy for paleoceanography. *Earth and Planetary Science Letters* 211, 159–171.

Swanner, E.D., Lambrecht, N., Wittkop, C., Harding, C., Katsev, S., Torgeson, J., Poulton, S.W. (2020) The biogeochemistry of ferruginous lakes and past ferruginous oceans. *Earth-Science Reviews* 211, 103430.

Tian, H. *et al.* (2015) Zircon LA-MC-ICPMS U-Pb dating of tuff from mesoproterozoic Gaoyuzhuang Formation in Jixian County of North China and its geological significance. *Acta Geoscientica Sinica* 36, 647–658 (in Chinese with English abstract).

Wang, X., Zhang, S., Wang, H., Bjerrum, C.J., Hammarlund, E.U., Haxen, E.R., Su, J., Wang, Y., Canfield, D.E. (2017) Oxygen, climate and the chemical evolution of a 1400 million year old tropical marine setting. *American Journal of Science* 317, 861–900.

Zhang, K., Zhu, X., Wood, R.A., Shi, Y., Gao, Z., Poulton, S.W. (2018) Oxygenation of the Mesoproterozoic ocean and the evolution of complex eukaryotes. *Nature Geoscience* 11, 345–350.

Zhang, S. *et al.* (2016) Sufficient oxygen for animal respiration 1,400 million years ago. *Proceedings of the National Academy of Sciences* 113, 1731–1736.

Zhu, S., Zhu, M., Knoll, A.H., Yin, Z., Zhao, F., Sun, S., Qu, Y., Shi, M., Liu, H. (2016) Decimetre-scale multicellular eukaryotes from the 1.56-billion-year-old Gaoyuzhuang Formation in North China. *Nature Communications* 7, 11500.

Geochemical Perspectives Letters

Black shale Mo isotope record reveals dynamic ocean redox during the Mesoproterozoic Era

Y. Ye, S. Zhang, H. Wang, X. Wang, C. Tan, M. Li, C. Wu, D.E. Canfield

Supplementary Information

The Supplementary Information includes:

- Methods
- Tables S-1 to S-4
- Figures S-1 to S-3
- Supplementary Information References

Methods

Elemental and TOC measurements

Major and trace elements were determined at the Analytical Laboratory of Beijing Research Institute of Uranium Geology, China National Nuclear Corporation, after methods of Zhang *et al.* (2015). Briefly, major elements were determined using a Philips PW2400 X-ray fluorescence spectrometer (XRF), while trace elements were obtained on an ELEMENT XR inductively coupled plasma mass spectrometer (ICP-MS) after rock powders were subjected to acid digestion. The resulting relative standard deviation (RSD) was <1.5 %.

Samples for TOC measurement were de-carbonated and combusted in a LECO CS-230HC carbon/sulfur analyser at the Key Laboratory of Petroleum Geochemistry, China National Petroleum Corporation. The RSD of TOC was <1 %.

Iron speciation

Iron speciation technique distinguishes four different Fe pools: carbonate Fe (Fe_{carb}), ferric oxide (Fe_{ox}), magnetite (Fe_{mag}), and pyrite (Fe_{py}). The former three species were sequentially extracted with acetate, dithionite, and oxalate (Poulton and Canfield, 2005), and then quantified with a SHIMADZU AA-7000 atomic adsorption spectrophotometer (AAS). Pyrite was extracted by Cr reduction, trapped as Ag_2S, with concentrations calculated gravimetrically (Canfield *et al.*, 1986). Replicate extractions of PACS-2 and in-house standards indicated analytical uncertainty of <5 %. These experiments were conducted at the University of Southern Denmark. The sum of the four reactive Fe phases gives the total concentration of highly reactive Fe (Fe_{HR}).

Molybdenum isotope analysis

Molybdenum isotope purification and analyses were completed at the State Key Laboratory of Ore Deposit Geochemistry, Institute of Geochemistry, Chinese Academy of Sciences, employing process outlined by Wen *et al.* (2010, 2011). Depending on Mo content, adequate amounts of ^{100}Mo–^{97}Mo double spike were added to each sample. An improved anion and column procedure was used to separate Mo (Zhang *et al.*, 2009). Isotope ratios were measured on a Neptune Plus multi-collector ICP-MS (MC-ICP-MS). Our δ^{98}Mo values are presented relative to the NIST SRM 3134 standard set to 0.25 ‰ (Nägler *et al.*, 2014):

$$\delta^{98}\mathrm{Mo} = \left(\left({}^{98/95}\mathrm{Mo}_{\mathrm{sample}}/\left({}^{98/95}\mathrm{Mo}_{\mathrm{NIST\text{-}3134}} \times 0.99975\right) - 1\right) \times 1000 \right. \quad \text{(S-1)}$$

Repeated evaluations of a pure NIST 3134 Mo solution and a mixture of NIST SRM 3134 and ^{100}Mo–^{97}Mo double spike (1:1) yielded reproducibilities of 0.09 ‰ and 0.06 ‰ (2 s.d.), respectively. Two artificially fractionated Mo solutions (SC2 and SC3) of Sigma-Aldrich Mo (lot 207306) gave average δ^{98}Mo values of 1.59 ± 0.09 ‰ (2 s.d., n = 12) and −1.68 ± 0.06 ‰ (n = 10), respectively, in line with the recommended values of 1.67 ‰ and −1.63 ‰ (Wen *et al.*, 2010). Analyses of the the USGS basalt standard powder (BCR-2) generated mean δ^{98}Mo of 0.22 ± 0.09 ‰ (n = 12), consistent with the reported value of 0.21 ‰ by Skierszkan *et al.* (2015). The results corrected by the double-spike method and the standard sample bracketing method agreed well with each other, and the external reproducibility was better than 0.1 ‰ for δ^{98}Mo.

Mass balance model

At steady state, the oceanic Mo isotope budget can be described as:

$$F_{\mathrm{in}} \times \delta_{\mathrm{in}} = F_{\mathrm{ox}} \times \delta_{\mathrm{ox}} + F_{\mathrm{red}} \times \delta_{\mathrm{red}} + F_{\mathrm{eux}} \times \delta_{\mathrm{eux}} \quad \text{(S-2)}$$

where the Mo outflux from seawater is determined by three redox settings: an oxic sink (ox), a euxinic sink (eux), and an intermediate reducing sink (inter). F_i and δ_i represent the Mo flux and isotope composition of each component (i).

The removal fluxes of redox sinks are defined as:

$$F_i = \mathrm{S} \times A_i \times b_i \quad \text{(S-3)}$$
$$A_{\mathrm{ox}} + A_{\mathrm{red}} + A_{\mathrm{eux}} = 1 \quad \text{(S-4)}$$
$$b_i = k \times b_{i\text{-today}} \quad \text{(S-5)}$$
$$k = [\mathrm{Mo}]_t/[\mathrm{Mo}]_{\mathrm{today}} \quad \text{(S-6)}$$

where S is the total seafloor area, A_i is the areal proportion of the sink, k is a reaction coefficient that relates burial efficiency (b_i) to oceanic Mo concentration ($[\mathrm{Mo}]_t$) and the modern average burial rate ($b_{i\text{-today}}$). Since changes in $[\mathrm{Mo}]_t$ will change b_i in a proportional manner, the reaction coefficient k will not affect the calculation.

The Mo isotope compositions of the three redox sinks can be expressed as:

$$\delta_i = \delta_{\mathrm{SW}} + \Delta_i \quad \text{(S-7)}$$

where δ_{SW} is the Mo isotopes of contemporaneous seawater and Δ_i represents the isotope fractionation associated with Mo removal into each redox sink. Combining the above equations, the seawater δ^{98}Mo in response to varying Mo sinks can be obtained. The parameters used in this model can be found in Scott *et al.* (2008).

Supplementary Tables

Table S-1 Geochemical data of the Gaoyuzhuang Formation (Member III).

The data table is available for download (Excel file) at https://www.geochemicalperspectivesletters.org/article2118.

Table S-2 Geochemical data of the Hongshuizhuang Formation.

The data table is available for download (Excel file) at https://www.geochemicalperspectivesletters.org/article2118.

Table S-3 Geochemical data of the Shennongjia Group.

The data table is available for download (Excel file) at https://www.geochemicalperspectivesletters.org/article2118.

Table S-4 Compilation of black shale Mo isotopes through geological time.

The data table is available for download (Excel file) at https://www.geochemicalperspectivesletters.org/article2118.

Supplementary Figures

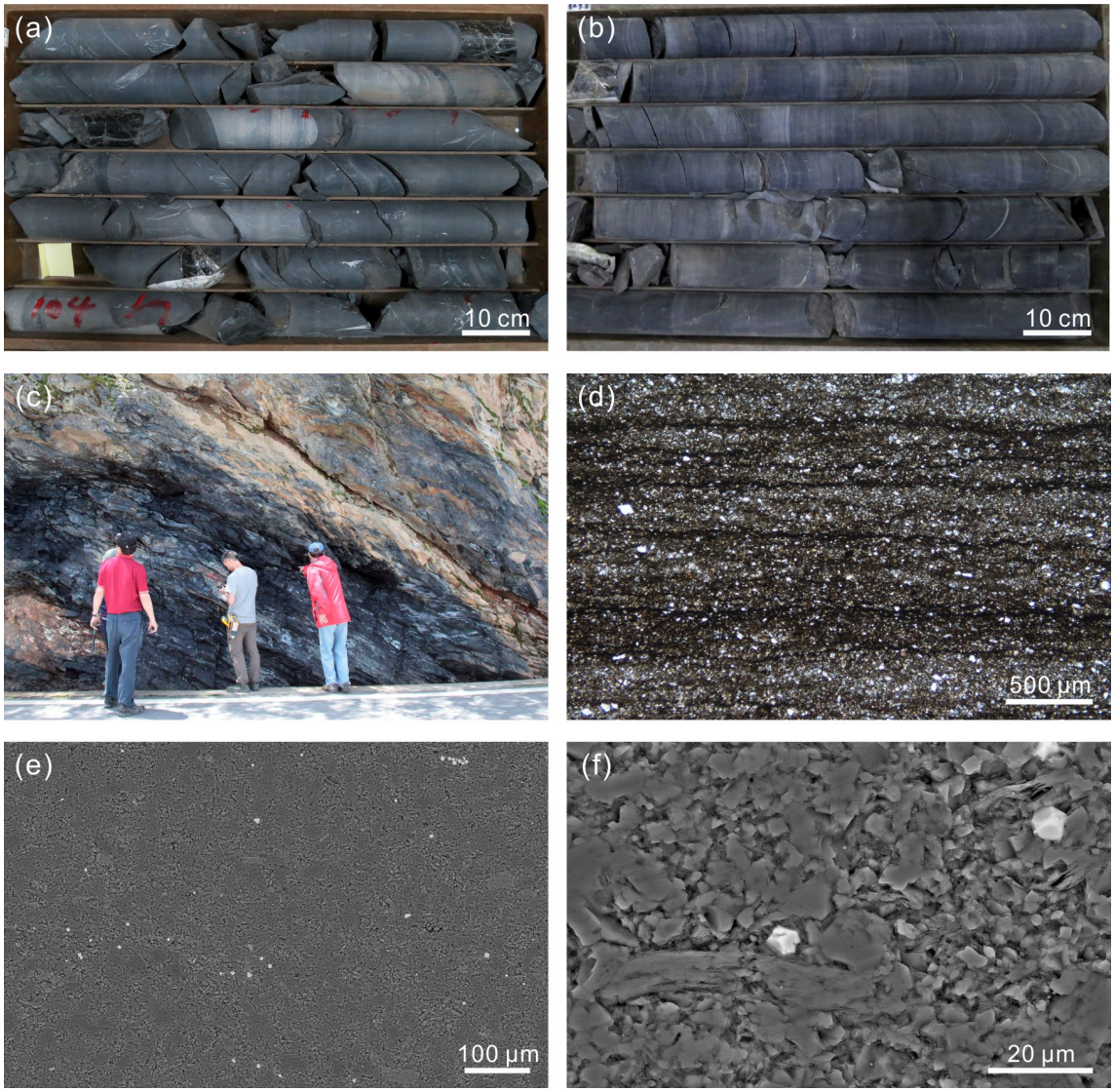

Figure S-1 Sedimentological observations of the studied units. **(a)** Core photo of organic-rich calcareous shales from the Gaoyuzhuang Formation (Member III), dip-corrected depth 167.8–169.7 m. **(b)** Core photo of the Hongshuizhuang shales, dip-corrected depth 405.8–409.8 m. **(c)** Outcrop of black shales from the Taizi Formation. **(d)** Thin section photomicrograph of sample from the Gaoyuzhuang Formation. **(e–f)** Representative backscattered electron images of the Gaoyuzhuang samples, showing the discrete distribution of pyrites.

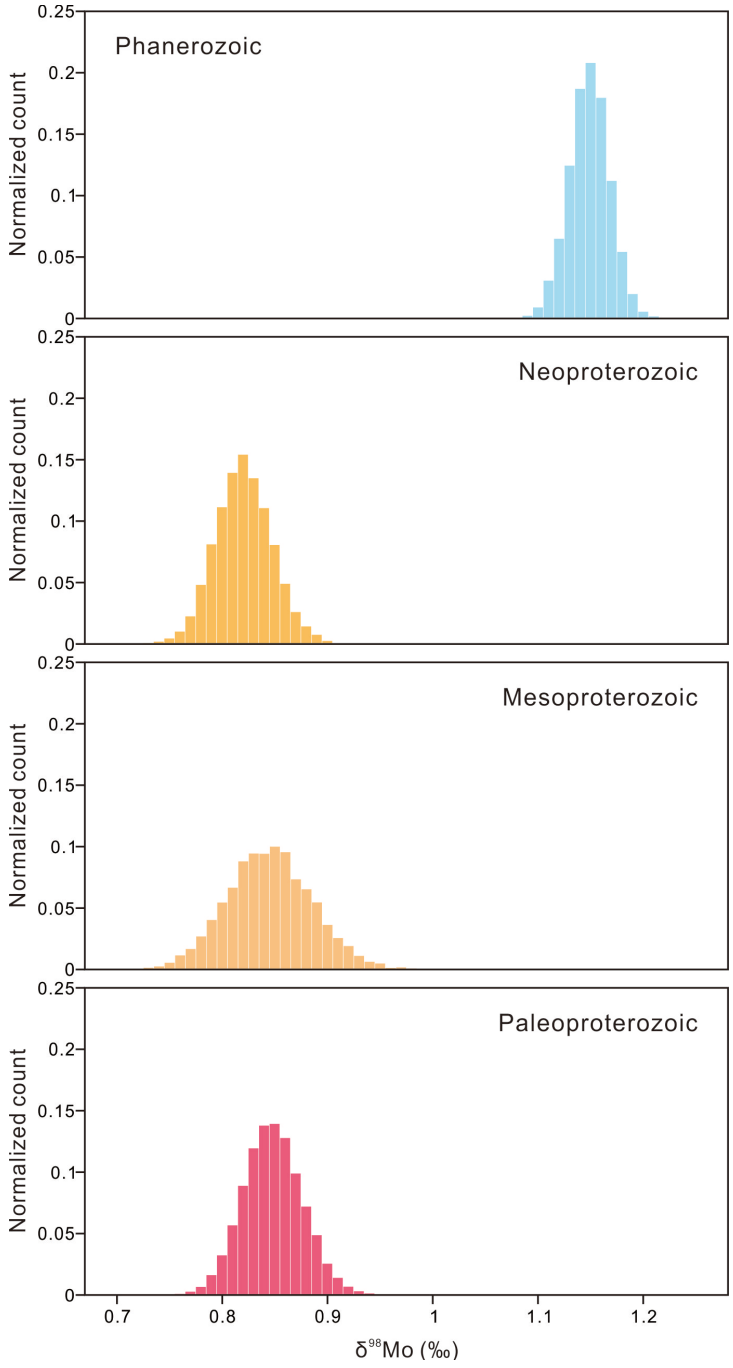

Figure S-2 Frequency distributions of bootstrap resampled δ^{98}Mo mean values (10,000 iterations) for the Paleoproterozoic, Mesoproterozoic, Neoproterozoic, and Phanerozoic samples with δ^{98}Mo > 0.3 ‰ (the continental crust composition; Voegelin *et al.*, 2014; Greaney *et al.*, 2020).

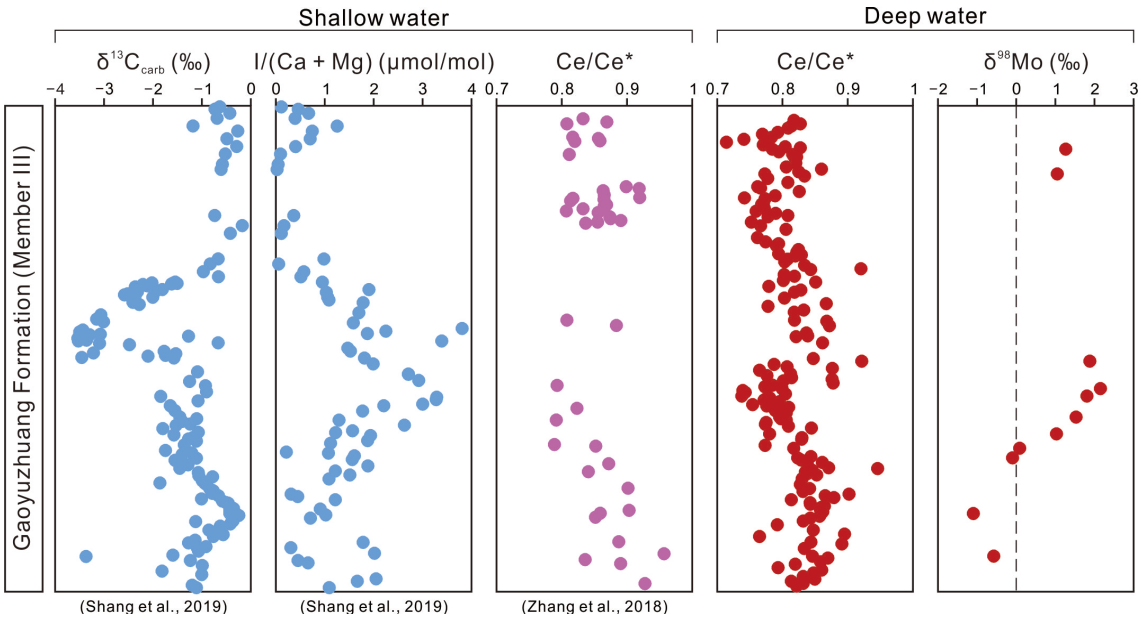

Figure S-3 Geochemical profiles of the Gaoyuzhuang Formation (Member III) at shallow- (Gangou and Jixian) and deep-water (this study) sections. The I/(Ca + Mg) ratios and carbonate carbon isotopes of the Gangou section are adopted from Shang *et al.* (2019). The Ce/Ce* values of the Jixian section are from Zhang *et al.* (2018). Ce/Ce* = $Ce_N/(Pr_N \times Pr_N/Nd_N)$ after Lawrence *et al.* (2006). The subscript "N" denotes normalization against Post-Archaean Average Shale (Taylor and McLennan, 1985).

Supplementary Information References

Arnold, G.L., Anbar, A.D., Barling, J., Lyons, T.W. (2004) Molybdenum Isotope Evidence for Widespread Anoxia in Mid-Proterozoic Oceans. *Science* 304, 87–90.

Asael, D., Rouxel, O., Poulton, S.W., Lyons, T.W., Bekker, A. (2018) Molybdenum record from black shales indicates oscillating atmospheric oxygen levels in the early paleoproterozoic. *American Journal of Science* 318, 275–299.

Asael, D., Tissot, F.L.H., Reinhard, C.T., Rouxel, O., Dauphas, N., Lyons, T.W., Ponzevera, E., Liorzou, C., Chéron, S. (2013) Coupled molybdenum, iron and uranium stable isotopes as oceanic paleoredox proxies during the Paleoproterozoic Shunga Event. *Chemical Geology* 362, 193–210.

Barling, J., Arnold, G.L., Anbar, A.D. (2001) Natural mass-dependent variations in the isotopic composition of molybdenum. *Earth and Planetary Science Letters* 193, 447–457.

Cabral, A.R. *et al.* (2013) Trace-element and multi-isotope geochemistry of Late-Archean black shales in the Carajás iron-ore district, Brazil. *Chemical Geology* 362, 91–104.

Canfield, D.E. *et al.* (2013) Oxygen dynamics in the aftermath of the Great Oxidation of Earth's atmosphere. *Proceedings of the National Academy of Sciences* 110, 16736–16741.

Canfield, D.E., Raiswell, R., Westrich, J.T., Reaves, C.M., Berner, R.A. (1986) The use of chromium reduction in the analysis of reduced inorganic sulfur in sediments and shales. *Chemical Geology* 54, 149–155.

Chen, J., Zhao, L., Algeo, T.J., Zhou, L., Zhang, L., Qiu, H. (2019) Evaluation of paleomarine redox conditions using Mo-isotope data in low-[Mo] sediments: A case study from the Lower Triassic of South China. *Palaeogeography, Palaeoclimatology, Palaeoecology* 519, 178–193.

Chen, X. *et al.* (2015) Rise to modern levels of ocean oxygenation coincided with the Cambrian radiation of animals. *Nature Communications* 6, 7142.

Cheng, M. *et al.* (2016) Marine Mo biogeochemistry in the context of dynamically euxinic mid-depth waters: A case study of the lower Cambrian Niutitang shales, South China. *Geochimica et Cosmochimica Acta* 183, 79–93.

Cheng, M. *et al.* (2017) Transient deep-water oxygenation in the early Cambrian Nanhua Basin, South China. *Geochimica et Cosmochimica Acta* 210, 42–58.

Cheng, M., Li, C., Chen, X., Zhou, L., Algeo, T.J., Ling, H.F., Feng, L.J., Jin, C.S. (2018) Delayed Neoproterozoic oceanic oxygenation: Evidence from Mo isotopes of the Cryogenian Datangpo Formation. *Precambrian Research* 319, 187–197.

Dahl, T.W. *et al.* (2010) Devonian rise in atmospheric oxygen correlated to the radiations of terrestrial plants and large predatory fish. *Proceedings of the National Academy of Sciences* 107, 17911–17915.

Dahl, T.W., Canfield, D.E., Rosing, M.T., Frei, R.E., Gordon, G.W., Knoll, A.H., Anbar, A.D. (2011) Molybdenum evidence for expansive sulfidic water masses in ~750 Ma oceans. *Earth and Planetary Science Letters* 311, 264–274.

Diamond, C.W., Planavsky, N.J., Wang, C., Lyons, T.W. (2018) What the ~1.4 Ga Xiamaling Formation can and cannot tell us about the mid-Proterozoic ocean. *Geobiology* 16, 219–236.

Dickson, A.J., Cohen, A.S. (2012) A molybdenum isotope record of Eocene Thermal Maximum 2: Implications for global ocean redox during the early Eocene. *Paleoceanography* 27, 1–9.

Dickson, A.J., Gill, B.C., Ruhl, M., Jenkyns, H.C., Porcelli, D., Idiz, E., Lyons, T.W., van den Boorn, S.H.J.M. (2017) Molybdenum-isotope chemostratigraphy and paleoceanography of the Toarcian Oceanic Anoxic Event (Early Jurassic). *Paleoceanography* 32, 813–829.

Duan, Y., Anbar, A.D., Arnold, G.L., Lyons, T.W., Gordon, G.W., Kendall, B. (2010) Molybdenum isotope evidence for mild environmental oxygenation before the Great Oxidation Event. *Geochimica et Cosmochimica Acta* 74, 6655–6668.

Eroglu, S., Scholz, F., Frank, M., Siebert, C. (2020) Influence of particulate versus diffusive molybdenum supply mechanisms on the molybdenum isotope composition of continental margin sediments. *Geochimica et Cosmochimica Acta* 273, 51–69.

Gilleaudeau, G.J., Sahoo, S.K., Ostrander, C.M., Owens, J.D., Poulton, S.W., Lyons, T.W., Anbar, A.D. (2020) Molybdenum isotope and trace metal signals in an iron-rich Mesoproterozoic ocean: A snapshot from the Vindhyan Basin, India. *Precambrian Research* 343, 105718.

Gordon, G.W., Lyons, T.W., Arnold, G.L., Roe, J., Sageman, B.B., Anbar, A.D. (2009) When do black shales tell molybdenum isotope tales? *Geology* 37, 535–538.

Greaney, A.T., Rudnick, R.L., Romaniello, S.J., Johnson, A.C., Gaschnig, R.M., Anbar, A.D. (2020) Molybdenum isotope fractionation in glacial diamictites tracks the onset of oxidative weathering of the continental crust. *Earth and Planetary Science Letters* 534, 116083.

Herrmann, A.D., Kendall, B., Algeo, T.J., Gordon, G.W., Wasylenki, L.E., Anbar, A.D. (2012) Anomalous molybdenum isotope trends in Upper Pennsylvanian euxinic facies: Significance for use of δ^{98}Mo as a global marine redox proxy. *Chemical Geology* 324–325, 87–98.

Kendall, B. *et al.* (2015) Uranium and molybdenum isotope evidence for an episode of widespread ocean oxygenation during the late Ediacaran period. *Geochimica et Cosmochimica Acta* 156, 173–193.

Kendall, B. *et al.* (2020) Inverse correlation between the molybdenum and uranium isotope compositions of Upper Devonian black shales caused by changes in local depositional conditions rather than global ocean redox variations. *Geochimica et Cosmochimica Acta* 287, 141–164.

Kendall, B., Creaser, R.A., Gordon, G.W., Anbar, A.D. (2009) Re-Os and Mo isotope systematics of black shales from the Middle Proterozoic Velkerri and Wollogorang Formations, McArthur Basin, northern Australia. *Geochimica et Cosmochimica Acta* 73, 2534–2558.

Kendall, B., Gordon, G.W., Poulton, S.W., Anbar, A.D. (2011) Molybdenum isotope constraints on the extent of late Paleoproterozoic ocean euxinia. *Earth and Planetary Science Letters* 307, 450–460.

Kurzweil, F., Drost, K., Pašava, J., Wille, M., Taubald, H., Schoeckle, D., Schoenberg, R. (2015a) Coupled sulfur, iron and molybdenum isotope data from black shales of the Teplá-Barrandian unit argue against deep ocean oxygenation during the Ediacaran. *Geochimica et Cosmochimica Acta* 171, 121–142.

Kurzweil, F., Wille, M., Schoenberg, R., Taubald, H., Van Kranendonk, M.J. (2015b) Continuously increasing δ^{98}Mo values in Neoarchean black shales and iron formations from the Hamersley Basin. *Geochimica et Cosmochimica Acta* 164, 523–542.

Lawrence, M.G., Greig, A., Collerson, K.D., Kamber, B.S. (2006) Rare earth element and yttrium variability in South East Queensland waterways. *Aquatic Geochemistry* 12, 39–72.

Lehmann, B., Nägler, T.F., Holland, H.D., Wille, M., Mao, J., Pan, J., Ma, D., Dulski, P. (2007) Highly metalliferous carbonaceous shale and Early Cambrian seawater. *Geology* 35, 403–406.

Nägler, T.F., Anbar, A.D., Archer, C., Goldberg, T., Gordon, G.W., Greber, N.D., Siebert, C., Sohrin, Y., Vance, D. (2014) Proposal for an international molybdenum isotope measurement standard and data representation. *Geostandards and Geoanalytical Research* 38, 149–151.

Neubert, N., Nägler, T.F., Böttcher, M.E. (2008) Sulfidity controls molybdenum isotope fractionation into euxinic sediments: Evidence from the modern Black Sea. *Geology* 36, 775–778.

Noordmann, J., Weyer, S., Montoya-Pino, C., Dellwig, O., Neubert, N., Eckert, S. (2015) Uranium and molybdenum isotope systematics in modern euxinic basins: Case studies from the central Baltic Sea and the Kyllaren fjord (Norway). *Chemical Geology* 396, 182–195.

Ossa Ossa, F., Hofmann, A., Wille, M., Spangenberg, J.E., Bekker, A., Poulton, S.W., Eickmann, B., Schoenberg, R. (2018) Aerobic iron and manganese cycling in a redox-stratified Mesoarchean epicontinental sea. *Earth and Planetary Science Letters* 500, 28–40.

Ostrander, C.M. *et al.* (2019a) Multiple negative molybdenum isotope excursions in the Doushantuo Formation (South China) fingerprint complex redox-related processes in the Ediacaran Nanhua Basin. *Geochimica et Cosmochimica Acta* 261, 191–209.

Ostrander, C.M. *et al.* (2020) An expanded shale δ^{98}Mo record permits recurrent shallow marine oxygenation during the Neoarchean. *Chemical Geology* 532, 119391.

Ostrander, C.M., Nielsen, S.G., Owens, J.D., Kendall, B., Gordon, G.W., Romaniello, S.J., Anbar, A.D. (2019b) Fully oxygenated water columns over continental shelves before the Great Oxidation Event. *Nature Geoscience* 12, 186–191.

Pearce, C.R., Cohen, A.S., Coe, A.L., Burton, K.W. (2008) Molybdenum isotope evidence for global ocean anoxia coupled with perturbations to the carbon cycle during the early Jurassic. *Geology* 36, 231–234.

Planavsky, N.J. *et al.* (2018) Evidence for episodic oxygenation in a weakly redox-buffered deep mid-Proterozoic ocean. *Chemical Geology* 483, 581–594.

Poulton, S.W., Canfield, D.E. (2005) Development of a sequential extraction procedure for iron: Implications for iron partitioning in continentally derived particulates. *Chemical Geology* 214, 209–221.

Proemse, B.C., Grasby, S.E., Wieser, M.E., Mayer, B., Beauchamp, B. (2013) Molybdenum isotopic evidence for oxic marine conditions during the latest Permian extinction. *Geology* 41, 967–970.

Scheller, E.L., Dickson, A.J., Canfield, D.E., Korte, C., Kristiansen, K.K., Dahl, T.W. (2018) Ocean redox conditions between the snowballs – Geochemical constraints from Arena Formation, East Greenland. *Precambrian Research* 319, 173–186.

Scholz, F., Siebert, C., Dale, A.W., Frank, M. (2017) Intense molybdenum accumulation in sediments underneath a nitrogenous water column and implications for the reconstruction of paleo-redox conditions based on molybdenum isotopes. *Geochimica et Cosmochimica Acta* 213, 400–417.

Scott, C., Lyons, T.W., Bekker, A., Shen, Y., Poulton, S.W., Chu, X., Anbar, A.D. (2008) Tracing the stepwise oxygenation of the Proterozoic ocean. *Nature* 452, 456–459.

Shang, M., Tang, D., Shi, X., Zhou, L., Zhou, X., Song, H., Jiang, G. (2019) A pulse of oxygen increase in the early Mesoproterozoic ocean at ca. 1.57–1.56 Ga. *Earth and Planetary Science Letters* 527, 115797.

Siebert, C., Kramers, J.D., Meisel, T., Morel, P., Nägler, T.F. (2005) PGE, Re-Os, and Mo isotope systematics in Archean and early Proterozoic sedimentary systems as proxies for redox conditions of the early Earth. *Geochimica et Cosmochimica Acta* 69, 1787–1801.

Skierszkan, E.K., Amini, M., Weis, D. (2015) A practical guide for the design and implementation of the double-spike technique for precise determination of molybdenum isotope compositions of environmental samples. *Analytical and Bioanalytical Chemistry* 407, 1925–1935.

Stockey, R.G., Sperling, E.A., Cole, D.B. (2020) Persistent global marine euxinia in the early Silurian. *Nature Communications* 11, 1804.

Taylor, S.R., McLennan, S.M. (1985) *The Continental Crust: its Composition and Evolution*. Blackwell, Oxford.

Voegelin, A.R., Pettke, T., Greber, N.D., von Niederhäusern, B., Nägler, T.F. (2014) Magma differentiation fractionates Mo isotope ratios: Evidence from the Kos Plateau Tuff (Aegean Arc). *Lithos* 190–191, 440–448.

Wegwerth, A. *et al.* (2018) Redox evolution during Eemian and Holocene sapropel formation in the Black Sea. *Palaeogeography, Palaeoclimatology, Palaeoecology* 489, 249–260.

Wen, H., Carignan, J., Cloquet, C., Zhu, X., Zhang, Y. (2010) Isotopic delta values of molybdenum standard reference and prepared solutions measured by MC-ICP-MS: Proposition for delta zero and secondary references. *Journal of Analytical Atomic Spectrometry* 25, 716–721.

Wen, H., Carignan, J., Zhang, Y., Fan, H., Cloquet, C., Liu, S. (2011) Molybdenum isotopic records across the Precambrian-Cambrian boundary. *Geology* 39, 775–778.

Wen, H., Fan, H., Zhang, Y., Cloquet, C., Carignan, J. (2015) Reconstruction of early Cambrian ocean chemistry from Mo isotopes. *Geochimica et Cosmochimica Acta* 164, 1–16.

Westermann, S., Vance, D., Cameron, V., Archer, C., Robinson, S.A. (2014) Heterogeneous oxygenation states in the Atlantic and Tethys oceans during Oceanic Anoxic Event 2. *Earth and Planetary Science Letters* 404, 178–189.

Wille, M., Kramers, J.D., Nägler, T.F., Beukes, N.J., Schröder, S., Meisel, T., Lacassie, J.P., Voegelin, A.R. (2007) Evidence for a gradual rise of oxygen between 2.6 and 2.5 Ga from Mo isotopes and Re-PGE signatures in shales. *Geochimica et Cosmochimica Acta* 71, 2417–2435.

Wille, M., Nägler, T.F., Lehmann, B., Schröder, S., Kramers, J.D. (2008) Hydrogen sulphide release to surface waters at the Precambrian/Cambrian boundary. *Nature* 453, 767–769.

Wille, M., Nebel, O., Van Kranendonk, M.J., Schoenberg, R., Kleinhanns, I.C., Ellwood, M.J. (2013) Mo-Cr isotope evidence for a reducing Archean atmosphere in 3.46-2.76 Ga black shales from the Pilbara, Western Australia. *Chemical Geology* 340, 68–76.

Xu, L., Lehmann, B., Mao, J., Nägler, T.F., Neubert, N., Böttcher, M.E., Escher, P. (2012) Mo isotope and trace element patterns of Lower Cambrian black shales in South China: Multi-proxy constraints on the paleoenvironment. *Chemical Geology* 318–319, 45–59.

Ye, Y., Wang, H., Wang, X., Zhai, L., Wu, C., Canfield, D.E., Zhang, S. (2020) Tracking the evolution of seawater Mo isotopes through the Ediacaran–Cambrian transition. *Precambrian Research* 350, 105929.

Yin, L., Li, J., Tian, H., Long, X. (2018) Rhenium–osmium and molybdenum isotope systematics of black shales from the Lower Cambrian Niutitang Formation, SW China: Evidence of a well oxygenated ocean at ca. 520 Ma. *Chemical Geology* 499, 26–42.

Zhang, K., Zhu, X., Wood, R.A., Shi, Y., Gao, Z., Poulton, S.W. (2018) Oxygenation of the Mesoproterozoic ocean and the evolution of complex eukaryotes. *Nature Geoscience* 11, 345–350.

Zhang, S. *et al.* (2015) Orbital forcing of climate 1.4 billion years ago. *Proceedings of the National Academy of Sciences* 112, E1406–E1413.

Zhang, Y., Wen, H., Fan, H. (2009) Chemical pretreatment methods for measurement of Mo isotope ratio on geological samples. *Chinese Journal of Analytical Chemistry* 2, 216–220 (in Chinese with English abstract).

Zhou, L., Su, J., Huang, J.H., Yan, J.X., Xie, X.N., Gao, S., Dai, M.N., Tonger (2011) A new paleoenvironmental index for anoxic events-Mo isotopes in black shales from Upper Yangtze marine sediments. *Science China Earth Sciences* 54, 1024–1033.